Role of Aromatic Interactions in Amyloid Formation by Peptides Derived from Human Amylin†

Sylvia M. Tracz,‡,§ Andisheh Abedini,‡,§ Miles Driscoll,§ and Daniel P. Raleigh*,§,||

Department of Chemistry, and Graduate Program in Biochemistry and Structural Biology, Graduate Program in Biophysics, State University of New York at Stony Brook, Stony Brook, New York 11794

Received June 8, 2004; Revised Manuscript Received September 27, 2004

ABSTRACT: Numerous polypeptides and proteins form amyloid deposits *in vivo* or *in vitro*. The mechanism of amyloid formation is not well-understood particularly in the case where unstructured polypeptides assemble to form amyloid. Aromatic−aromatic interactions are known to be important in globular proteins, and the possibility that they might play a key role in amyloid formation has been raised. The results of Ala-scanning experiments on short polypeptides derived from Amylin have suggested that aromatic interactions could be particularly important for this system. Here, we examine a set of Amylin-derived polypeptides in which the single aromatic residue has been substituted with a Leu and Ala. A peptide corresponding to residues 21−29 with a Phe-23 to Leu substitution, a free N terminus, and amidated C terminus readily forms amyloid. Shorter peptides derived from the putative minimal amyloid-forming segment of Amylin, residues 22−27, also form amyloid when Phe-23 is replaced by Leu. Amyloid formation is more facile when the N terminus is deprotonated and the peptide is uncharged. Substitution of the Phe with Ala results in a peptide that is noticeably less prone to form amyloid. A peptide corresponding to residues 10−19 of human Amylin with blocked termini and the sole aromatic residue, Phe-15, substituted by Leu readily forms amyloid. A Phe-15 to Ala substitution reduces significantly the ability to form amyloid. These results indicate that an aromatic residue is not required for amyloid formation in these systems and indicates that other factors such as size, β-sheet propensity, and hydrophobicity of the side chain in question are also important.

A growing number of polypeptides and proteins have been shown to form partially structured deposits known as amyloid either *in vitro* or *in vivo*. Amyloid fibrils are rich in β-sheet structure and are characteristically long and narrow, typically 10 nm in width, and unbranched (*1*). Amyloid deposits are often cytotoxic and are thought to contribute to the pathology of a number of diseases *in vivo*, including Alzheimer's disease, familial amyloidoses, and type 2 diabetes mellitus (*1*−*4*). From a structural perspective, the process of amyloid formation can be roughly divided into two classes. On one hand, there are a number of globular proteins that self-assemble to form amyloid starting from a folded or partially folded state. The second class consists of polypeptides that lack definite globular structure in their unaggregated state. Prominent examples of this class include Amylin, also known as islet amyloid polypeptide (IAPP),[1] the polypeptide responsible for amyloid formation in type 2 diabetes, and Aβ-amyloid, the proteolytic fragment that forms amyloid deposits in Alzheimer's disease (*5*−*9*). The pathway of amyloid formation is not understood in detail despite its obvious importance. This is particularly true for amyloid formation by unstructured or partially structured polypeptides.

Elucidating the specific interactions and patterns of residues that stabilize amyloid fibrils and guide their self-assembly is a key step in developing strategies to inhibit and control fibril formation (*10*−*14*). A range of short protein fragments derived from unrelated amyloid-forming proteins have been found to contain aromatic residues. Aromatic−aromatic interactions are known to be important in globular proteins (*15*), and recent experimental studies have lead to the interesting suggestion that interactions between aromatic residues play a key role in fibril formation by polypeptides (*12*, *16*−*18*). These studies involved alanine-scanning ex-

† This work was supported by NIH Grant GM54233 to D.P.R.

* To whom correspondence should be addressed: State University of New York at Stony Brook, Stony Brook, NY 11794. Phone: (631) 632-9547. Fax: (631) 632-7960. E-mail: draleigh@notes.cc.sunysb.edu.

‡ The first two authors contributed equally to this work.

§ Department of Chemistry.

|| Graduate Program in Biochemistry and Structural Biology, Graduate Program in Biophysics.

[1] Abbreviations: DIPEA, *N*,*N*-diisopropylethylamine; DMF, *N*,*N*-dimethylformamide; Fmoc, 9-fluorenylmethoxycarbonyl; FTIR, Fourier transform infrared; hAmylin$_{21-29}$ F23L, residues 21−29 of human Amylin with an amidated C terminus containing a Phe-23 to Leu substitution; hAmylin$_{22-27}$ F23L, residues 22−27 of human Amylin with an amidated C terminus containing a Phe-23 to Leu substitution; hAmylin$_{22-27}$ F23A, residues 22−27 of human Amylin with an amidated C terminus containing a Phe-23 to Ala substitution; hAmylin$_{10-19}$ F15L, residues 10−19 of human Amylin with an amidated C terminus and acetylated N terminus containing a Phe-15 to Leu substitution; hAmylin$_{10-19}$ F15A, residues 10−19 of human Amylin with an amidated C terminus and acetylated N terminus containing a Phe-15 to Ala substitution; hAmylin$_{10-19}$ H18A, residues 10−19 of human Amylin with an amidated C terminus and acetylated N terminus containing a His-18 to Ala substitution; HBTU, *O*-benzotriazol-1-yl-*N*,*N*,*N*′,*N*′-tetramethyluronium hexafluorophosphate; HOBT, *N*-hydroxybenzotriazole monohydrate; HPLC, high-performance liquid chromatography; IAPP, islet amyloid polypeptide; MALDI−TOF MS, matrix-assisted laser desorption ionization−time-of-flight mass spectrometry; PAL-PEG, 5-(4′-Fmoc-aminomethyl-3′,5-dimethoxyphenol)-valeric acid; TEM, transmission electron microscopy; TFA, trifluoroacetic acid; v/v, volume/volume.

10.1021/bi048812l CCC: $27.50
Published on Web 11/18/2004

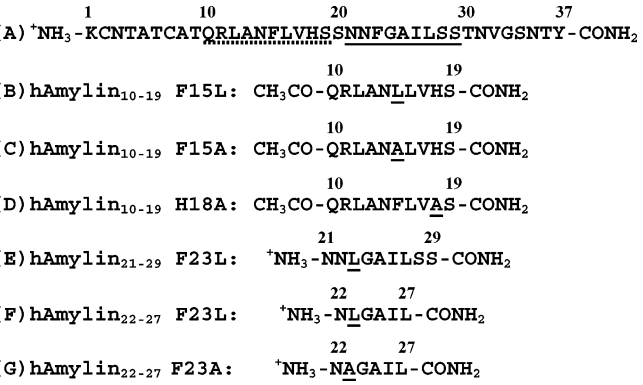

FIGURE 1: (A) Primary sequence of human Amylin. Residues 10−19 are underlined with a dashed line, and residues 21−29 are underlined with a solid line. The naturally occurring protein has a disulfide bridge between Cys-2 and Cys-7 and an amidated C terminus. (B) F15L variant of the 10−19 fragment, $hAmylin_{10-19}$ F15L. (C) F15A variant of the 10−19 fragment, $hAmylin_{10-19}$ F15A. (D) H18A variant of the 10−19 fragment, $hAmylin_{10-19}$ H18A. (E) F23L variant of the 21−29 fragment, $hAmylin_{21-29}$ F23L. (F) F23L variant of the 22−27 fragment, $hAmylin_{22-27}$ F23L. (G) F23A variant of the 22−27 fragment, $hAmylin_{22-27}$ F23A. Residues are numbered according to their position in full-length Amylin. The position of the Phe or His in the wild-type sequence is underlined in all of the peptides. All of the peptides from the 10−19 region have an acetylated N terminus, while the peptides derived from the 21−29 and 22−27 regions have a free N terminus. All variants have an amidated C terminus.

periments and focused on small polypeptides derived from Amylin and Calcitonin (*16*, *18*). In contrast, strategies for predicting the intrinsic effects of mutations on the rate of aggregation of unstructured polypeptides have been reasonably successful without including aromatic−aromatic interactions (*11*). In this work, we examine the role of aromatic−aromatic interactions in more detail and show that they are in fact not required for amyloid formation by a set of Amylin-derived peptides.

Amylin is a normally soluble 37-residue polypeptide hormone. It is produced in the pancreatic β-cells and is cosecreted with insulin (*5*, *8*, *9*, *19*). In its soluble form the polypeptide plays a role in glucose homeostasis (*20*−*22*). In type 2 diabetes mellitus, Amylin aggregates in the islet extracellular space to form amyloid deposits in more then 95% of patients with the disease (*5*, *8*, *21*, *22*). The sequence of Amylin is shown in Figure 1.

Not all species form islet amyloid, and a comparison of the primary structure of Amylin from a number of organisms initially focused attention on the region encompassing residues 20−29. Early work suggested that this region was a key determinant of amyloid-forming ability and demonstrated that a peptide fragment corresponding to residues 20−29 of human Amylin is capable of forming amyloid *in vitro* (*23*). Studies with a large number of variants of the 20−29 fragment, including a systematic set of proline substitutions, have helped to pinpoint residues that appear to be important for amyloid formation in this system (*23*−*26*). Other regions of Amylin have been examined, and peptides corresponding to residues 8−20, 10−19, 20−29, 30−37, and 8−37 of human Amylin all form amyloid (*23*, *27*−*30*). Although the 20−29 segment is not the only amyloidogenic region in human Amylin, it is widely used as a model system for biophysical and computational studies of amyloid formation (*23*, *25*, *30*−*33*). Smaller peptides derived from this region have also been shown to form amyloid, and recent investigations have lead to the suggestion that the minimal amyloid-forming fragment of Amylin consists of residues 22−27 (*30*). This hexapeptide fragment, NFGAIL, forms β-sheet-containing fibrils that coil around each other in typical amyloid fibril morphology. A systematic alanine scan of the 22−27 hexapeptide revealed that substitution of Phe-23 with Ala abolishes the ability to form amyloid (*16*). In another study, aromatic interactions were proposed to play an important role in amyloid formation by short peptides derived from the region corresponding to residues 11−20 of human Amylin (*12*).

Here, we test the importance of aromatic−aromatic interactions in amyloid formation in more detail by examining a set of variant peptides derived from the 10−19 and 21−29 regions of human Amylin. These variants include a nine-residue peptide corresponding to residues 21−29, two hexapeptides corresponding to residues 22−27, as well as three decapeptides corresponding to residues 10−19. The consequences of substituting the single aromatic residue by Leu and Ala are examined. Our studies demonstrate that aromatic−aromatic interactions are not required for amyloid formation in these systems and by implication may not be rigorously required in other systems. Ala is obviously smaller than Leu or Phe, less hydrophobic, and has a smaller β-sheet propensity. Combinations of these factors likely influence the different behaviors of the Phe/Leu peptides versus the Ala peptides.

EXPERIMENTAL PROCEDURES

Peptide Synthesis and Purification. Peptides were synthesized on a 0.20 mmol scale on a Millipore 9050 Plus automated peptide synthesizer or on a 0.25 mmol scale using an Applied Biosystems 433A Peptide Synthesizer, using 9-fluornylmethoxycarbonyl (Fmoc) chemistry. Solvents used were ACS-grade. Reagents were purchased from Advanced Chemtech, PE Biosystems, Sigma, and Fisher Scientific. Use of a 5-(4′-Fmoc-aminomethyl-3′,5-dimethoxyphenol)valeric acid (PAL-PEG) resin afforded an amidated C terminus. Standard Fmoc reaction cycles were used. The first residue attached to the resin, all β-branched residues, and all residues directly following a β-branched residue were double-coupled. The crude peptides were purified via reverse-phase HPLC using a Vydac C18 preparative column. A two-buffer system was utilized. Buffer A consists of H_2O and 0.045% HCl (v/v). Buffer B consists of 80% acetonitrile, 20% H_2O, and 0.045% HCl (v/v). All peptides were analyzed by mass spectrometry using a Bruker MALDI−TOF MS to confirm their identity.

Fourier Transform Infrared (FTIR) Spectroscopy. Samples were prepared by dissolving each peptide in D_2O, incubating the solution at room temperature for 1 h, and then lyophilizing to remove residual water. The peptides were then redissolved in D_2O, and the pD was adjusted using DCl and NaOD. The same procedure was used to prepare samples for TEM and Congo Red staining. FTIR measurements were performed on a Biorad FTS-40A spectrometer using a DTGS detector with a 2 cm^{-1} resolution. A dismountable sample cell comprising CaF_2 plates and a 0.05 mm Teflon spacer was utilized. Interferograms were recorded from 4000 to 400

cm^{-1}. A total of 64 scans was taken with a 2 s delay. The interferograms were then averaged, and the solvent spectrum was subtracted. Samples were examined either as gels or as partially dried films.

Transmission Electron Microscopy (TEM). TEM was performed at the University Microscopy Imaging Center at the State University of New York at Stony Brook. A 4 μL sample was placed on a carbon-coated Formvar 200-mesh copper grid and negatively stained with saturated uranyl acetate.

Congo Red Staining and Birefringence. A 10 μL aliquot of the peptide sample was air-dried on a superfrost microscope slide and stained with an 80% ethanol solution saturated with sodium chloride and Congo Red. The slides were analyzed for amyloid formation using a Nikon SMZ-2T polarizing microscope.

RESULTS AND DISCUSSION

Design of Peptides. Three sets of variant peptides derived from two separate regions of human Amylin were synthesized and characterized. The first peptide is derived from the 21−29 residue region of human Amylin. We characterized a peptide corresponding to residues 21−29 with the sole aromatic residue Phe-23 substituted with Leu. This peptide is designated hAmylin$_{21-29}$ F23L. The respective wild-type peptide was also synthesized and is designated hAmylin$_{21-29}$ WT. Two variants derived from the putative minimal amyloid-forming fragment, residues 22−27, were also prepared. The first peptide is comprised of residues 22−27 of human Amylin where Phe-23 is replaced with leucine and is denoted hAmylin$_{22-27}$ F23L. The second peptide contains an alanine at position 23 and is designated hAmylin$_{22-27}$ F23A. The respective wild-type peptide was also synthesized and is denoted hAmylin$_{22-27}$ WT. All of the peptides were prepared with an amidated C terminus to avoid introducing an additional charged group and the N terminus was left free. None of the residues within the 21−29 block contains ionizable side chains; thus, the total net charge on our peptides can be varied from +1 at low pH, where the N terminus is protonated, to zero when the pH is raised above the pK_a of the N terminus.

The third set corresponds to residues 10−19 in which the sole aromatic residue, Phe-15, has been changed to either Leu or Ala. The peptides were prepared with an amidated C terminus and acetylated N terminus to avoid introducing extra charges. Acetylation of the N terminus also avoids potential problems with sample heterogeneity caused by the tendency of an N-terminal glutamine to cyclize to pyroglutamic acid. The only charged residues are Arg-11 and His-18. The peptide fragments are designated hAmylin$_{10-19}$ F15L and hAmylin$_{10-19}$ F15A. We also examined the role of the single His residue located at position 18 by studying a His-18 to Ala variant. This peptide is denoted hAmylin$_{10-19}$ H18A. The respective wild-type peptide was also synthesized and is denoted hAmylin$_{10-19}$ WT. The sequences of the peptides are listed in Figure 1. Note that the residues in all of the peptides are numbered according to their positions in full-length Amylin.

A Phe-23 to Leu Substitution in the 21−29 Fragment Does Not Prevent Amyloid Formation. Samples of hAmylin$_{21-29}$ WT and hAmylin$_{21-29}$ F23L were examined at pD 5.5 (±0.3) by FTIR spectroscopy, TEM, and Congo Red staining. FTIR spectra of freshly prepared solutions at pD 5.5 (±0.3) indicate the presence of significant β-sheet structure (Figure 2). There is an intense peak near 1620 cm^{-1} indicative of a β-sheet structure as well as a shoulder centered near 1645 cm^{-1}, a feature sometimes assigned to asparagine side chains and the protonated free N terminus. Bands for random coil and α-helix also fall near this region. TEM measurements confirmed the presence of amyloid fibrils with classic morphology (Figure 2). Congo Red staining experiments provided further evidence of amyloid formation. Samples were stained and viewed under a polarizing microscope. Birefringence was observed as expected for amyloid fibrils.

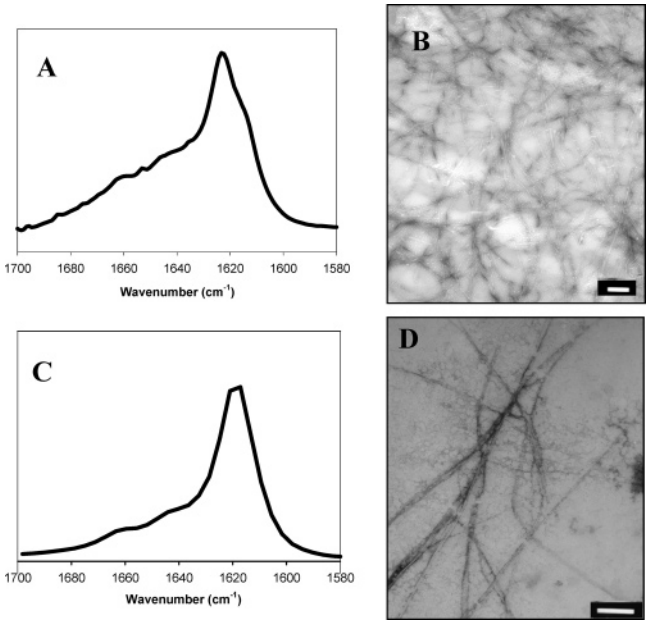

FIGURE 2: (A) FTIR spectrum and (B) TEM micrograph of hAmylin$_{21-29}$ WT at pD 5.5 (±0.3) collected immediately after sample preparation. The scale bar represents 200 nm. (C) FTIR spectrum and (D) TEM micrograph of hAmylin$_{21-29}$ F23L at pD 5.5 (±0.3) collected immediately after sample preparation. The scale bar represents 100 nm.

These results demonstrate that a Phe-23 to Leu substitution in the 21−29 region of IAPP does not eliminate amyloid formation. Both the variant, hAmylin$_{21-29}$ F23L, and the wild-type peptide form fibrils immediately upon sample preparation as indicated by FTIR and TEM (Figure 2). This peptide is three residues longer than the hexapeptide defined as the minimal amyloid-forming fragment, and it is possible that the additional residues provide interactions, which compensate for the Phe to Leu substitution. In other words, the shorter hexapeptide might be more sensitive to substitutions at position 23. Alternatively, as suggested by recent simulations, additional residues might alter the interstrand or intersheet packing so that Phe-Phe interactions are not as important (*32*). Consequently, we also examined the minimal amyloid-forming fragment, residues 22−27.

The hAmylin$_{22-27}$ F23L Variant Forms Amyloid at Low and High pH. The ability of the hAmylin$_{22-27}$ F23L peptide to form amyloid was compared to the wild-type sequence under conditions where the N terminus is charged (pD 5.5) and where it is neutral (pD ≥ 9.0). Samples were examined at 2 and 4 mg/mL to allow for a comparison with studies from other laboratories (*15*). The wild-type peptide formed

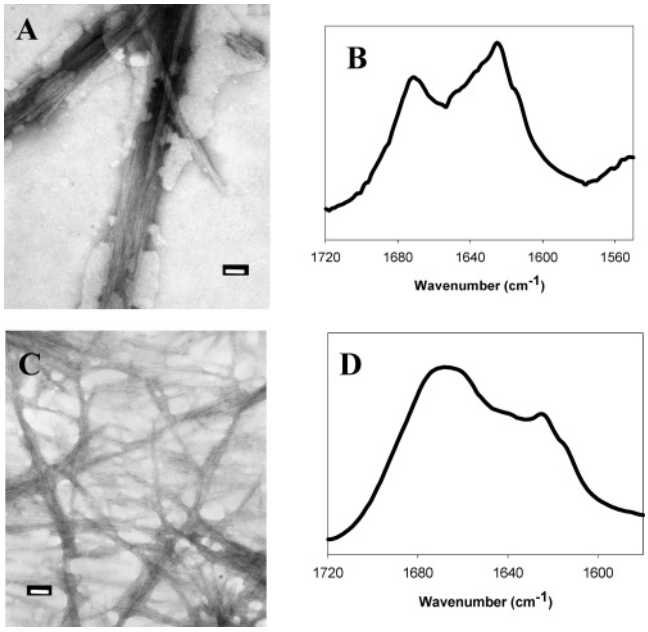

FIGURE 3: FTIR and TEM of hAmylin$_{22-27}$ WT at pD 5.5 (±0.3) and 9.0 (±0.3). TEM micrographs were collected immediately after sample preparation, and FTIR spectra were collected from samples dried overnight. (A) TEM micrograph at pD 5.5 (±0.3). (B) FTIR spectrum at pD 5.50 (±0.3). (C) TEM micrograph at pD 9.0 (±0.3). (D) FTIR spectrum at pD 9.0 (±0.3). The scale bars represent 50 nm.

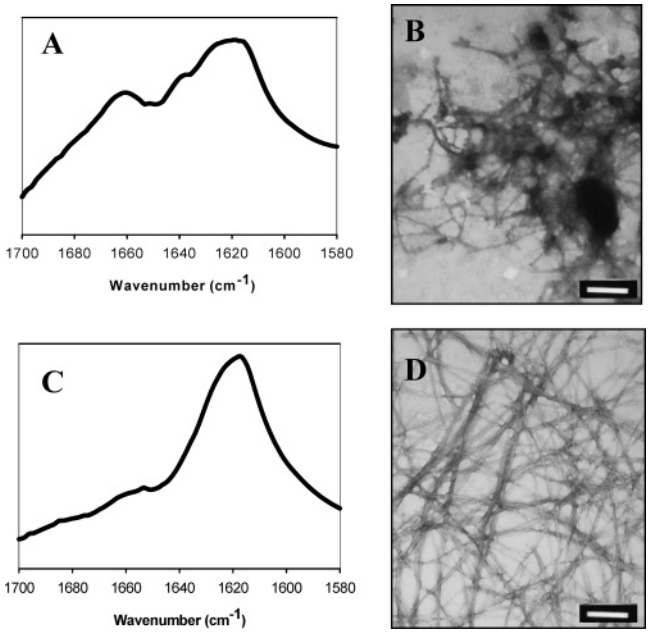

FIGURE 4: FTIR and TEM of hAmylin$_{22-27}$ F23L at pD 5.5 (±0.3) and 9.0 (±0.3). TEM micrographs were collected immediately after sample preparation, and FTIR spectra were collected from samples dried overnight. (A) FTIR spectrum at pD 5.50 (±0.3). (B) TEM micrograph at pD 5.5 (±0.3). (C) FTIR spectrum at pD 9.0 (±0.3). (D) TEM micrograph at pD 9.0 (±0.3). The scale bars represent 200 nm.

fibrils under both conditions as judged by TEM (Figure 3). The FTIR spectra exhibit multiple bands, but both spectra contain a band near 1625 cm^{-1} at pD 5.5 (±0.3) and pD 9.0 (±0.3) indicating a β-sheet structure (Figure 3). TEM of hAmylin$_{22-27}$ F23L revealed classic amyloid morphology broadly similar to the wild-type peptide (Figure 4). Amyloid fibrils were found in abundance and form clustered structures in the samples prepared at the higher concentration. There are some differences in the details of the micrographs recorded at low and high pD; however, both samples show the presence of amyloid fibrils. At pD 5.5 (±0.3), the fibrils aggregate and appear dense. At pD 9.0 (±0.3), they form unbranched ropelike assemblies. These experiments clearly demonstrate that an aromatic residue is not required for amyloid formation by this peptide. The samples of hAmylin$_{22-27}$ F23L examined at the lower concentration form more diffuse fibrils at both pD 5.5 (±0.3) and 9.0 (±0.3) (data not shown). At pD 5.5 (±0.3), the fibrils assemble into ropelike structures, while at pD 9.0 (±0.3) sheetlike assemblies are observed.

FTIR measurements and Congo Red staining experiments confirmed the presence of amyloid fibrils. The spectra of both the high and low concentration samples clearly indicate the presence of β-sheet secondary structure at both pD values; however, it appears more pronounced at the higher pD (Figure 4). At pD 5.5 (±0.3), the spectrum is dominated by a broad peak near 1620 cm^{-1} with a shoulder near 1640 cm^{-1}. At the higher pD 9.8 (±0.3), the peak at 1620 cm^{-1} is sharp. The spectra of the lower concentration sample displays a broad peak centered around 1627 cm^{-1}, at both high (5.40) and low (9.37) pD (data not shown). Interestingly, the β-sheet bands are relatively more intense in the hAmylin$_{22-27}$ F23L spectrum than in the wild-type spectrum. The origin of the differences is not clear but the important result is that the Phe to Leu variant readily forms amyloid. The samples were also examined by Congo Red staining. Both samples displayed the characteristic birefringence expected for amyloid deposits at both pH values.

We have previously shown that some peptides derived from IAPP can slowly deamidate in solution to produce small amounts of impurities that can affect the ability to aggregate (*34*). For example, impurities at the level of 5% or less were shown to induce aggregation in some proline-containing peptides derived from the 20−29 region of Amylin (*34*). Very low levels of impurities (1−2% or less as judged by analytical HPLC) were observed in the initial preparation of some samples. Repurification of the peptides to remove these low-level impurities had no effect upon amyloid formation. Thus, deamidation can be ruled out as contributing to aggregation.

This set of biophysical experiments demonstrates that hAmylin$_{22-27}$ F23L is capable of self-assembly into amyloid deposits. This indicates that a Phe at position 23 is not required to form amyloid fibrils.

The hAmylin$_{22-27}$ F23A Variant Is Less Prone to Form Amyloid than hAmylin$_{22-27}$ F23L. The results presented in the two previous sections show that a Phe-23 to Leu substitution does not prevent amyloid formation. The initial experiments on the role of Phe-23 involved substitution with Ala, and it is certainly possible that a less conservative Ala substitution could have a much larger effect then a Leu substitution (*16*). Consequently, samples of hAmylin$_{22-27}$ F23A were prepared and tested for amyloid formation using the same conditions employed for the hAmylin$_{22-27}$ F23L peptide. The peptide is much less prone to aggregate although it appears to have some tendency to aggregate and form deposits at high pH, which share some of the characteristics associated with amyloid.

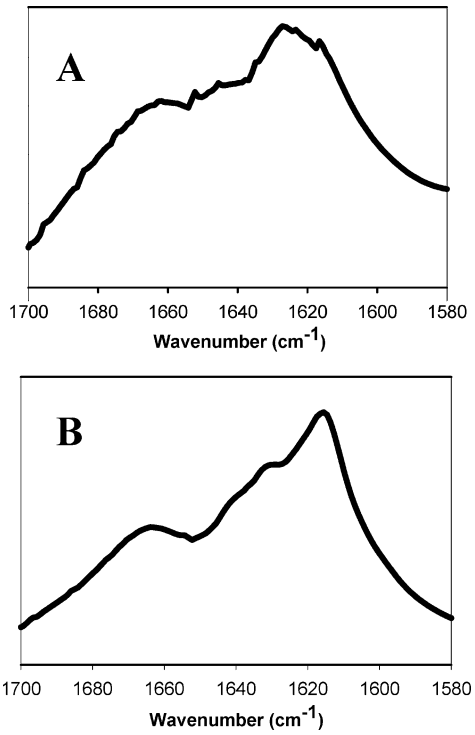

FIGURE 5: (A) FTIR spectrum of hAmylin$_{22-27}$ F23A recorded after 48 h of incubation at (A) pD 5.5 (±0.3) and (B) pD 9.0 (±0.3).

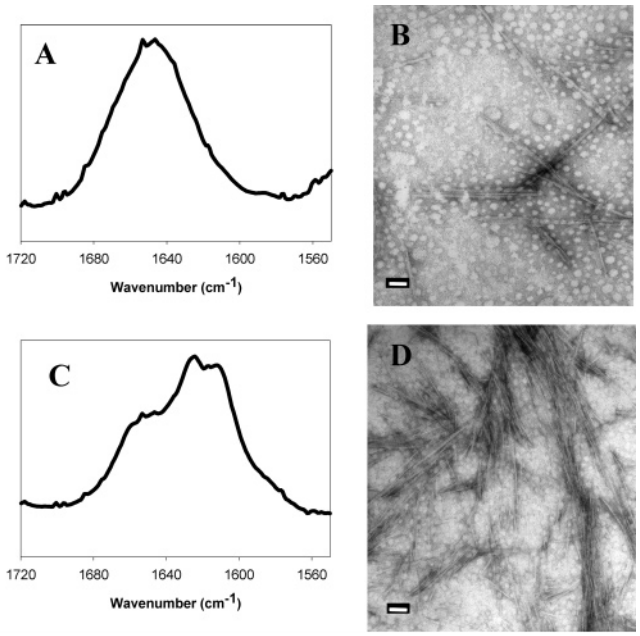

FIGURE 6: FTIR and TEM of hAmylin$_{10-19}$ WT at pD 4.0 (±0.3) and 9.0 (±0.3). (A) FTIR spectrum at pD 4.0 (±0.3) recorded after 3 h of incubation. (B) TEM micrograph collected 3 h after sample preparation at pD 4.0 (±0.3). (C) FTIR spectrum at pD 9.0 (±0.3) recorded after 3 h of incubation. (D) TEM micrograph collected 3 h after sample preparation at pD 9.0 (±0.3). The scale bars represent 50 nm.

FTIR spectra of hAymlin$_{22-27}$ F23A samples were recorded as partially dried films as is typical for short peptides (Figure 5). At pD 5.5 (±0.3) the spectrum displays a broad peak centered around 1625 cm^{-1} with a shoulder at 1645 cm^{-1} and a second broad peak near 1666 cm^{-1}. The spectrum recorded at pD 9.0 (±0.3) displayed a more prominate β-sheet peak at a low wavenumber. An intense peak is

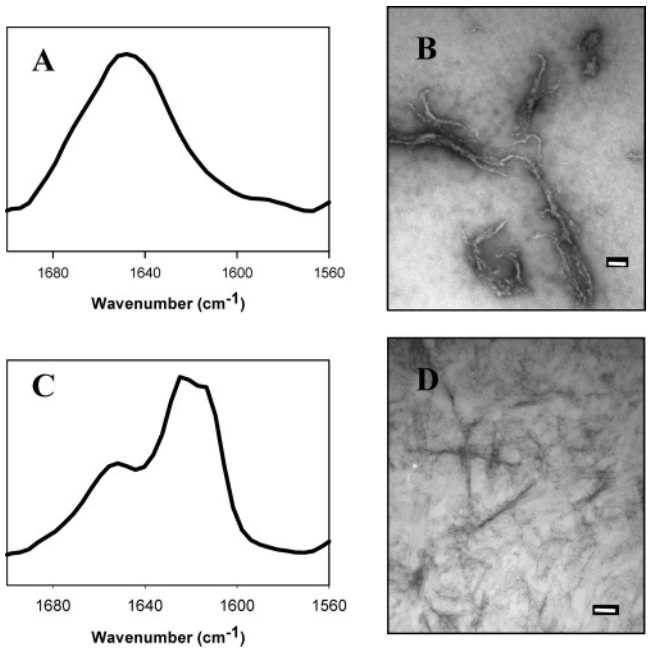

FIGURE 7: FTIR and TEM of hAmylin$_{10-19}$ F15L at pD 4.0 (±0.3) and 9.0 (±0.3). (A) FTIR at pD 4.0 (±0.3) recorded after 3 h of incubation. (B) TEM micrograph collected 3 h after sample preparation at pD 4.0 (±0.3). (C) FTIR spectrum at pD 9.0 (±0.3) recorded after 3 h of incubation. (D) TEM micrograph collected 3 h after sample preparation at pD 9.0 (±0.3). The scale bars represent 100 nm.

detected near 1620 cm^{-1}, and a less intense peak is present near 1666 cm^{-1}. Samples of hAmylin$_{22-27}$ F23A were analyzed with TEM. No fibrils were observed after 24 h at either pD 5.5 (±0.3) or 9.0 (±0.3). The solutions were tested again after 7 days, and no fibrils were found. Samples of hAmylin$_{22-27}$ F23A at pD 5.5 (±0.3) and 9.0 (±0.3) were stained and examined for birefringence. Birefringence was observed at both pD values; however, the hAmylin$_{22-27}$ F23A peptide exhibited less intense birefringence then the hAmylin$_{22-27}$ F23L peptide consistent with a reduced tendency to form amyloid.

To summarize, the hAmylin$_{22-27}$ F23L peptide clearly forms amyloid, while the hAmylin$_{22-27}$ F23A peptide gives more ambiguous results. The FTIR measurements and Congo Red staining experiments are consistent with formation of some partially ordered aggregates at high pH. In contrast, no fibrils were detected via TEM even after 7 days of incubation. When these measurements are taken together, they indicate that the Ala-substituted peptides are much less prone to form amyloid than the Leu-substituted peptides.

A Phe-15 to Leu Substitution in hAmylin$_{10-19}$ Does Not Prevent Amyloid Formation. The wild-type 10−19 fragment has been shown to form amyloid in a pH-dependent manner. Above the pK_a of the single His residue, the peptide readily aggregates to form amyloid as judged by FTIR, TEM, and Congo Red staining (*35*). Data for the wild-type peptide are presented in Figure 6. Fibrils are observed at both pD 4.0 (±0.3) and 9.0 (±0.3) by TEM but appear much more abundant at the higher pD. The FTIR spectrum recorded at pD 9.0 (±0.3) shows a peak near 1620 cm^{-1} consistent with β-sheet structure. In contrast, the spectrum recorded at pD 4 (±0.3) exhibits a broad peak near 1645 cm^{-1} (Figure 6). The FTIR spectra were recorded after incubating the sample for 3 h; however, the same features were observed after 24

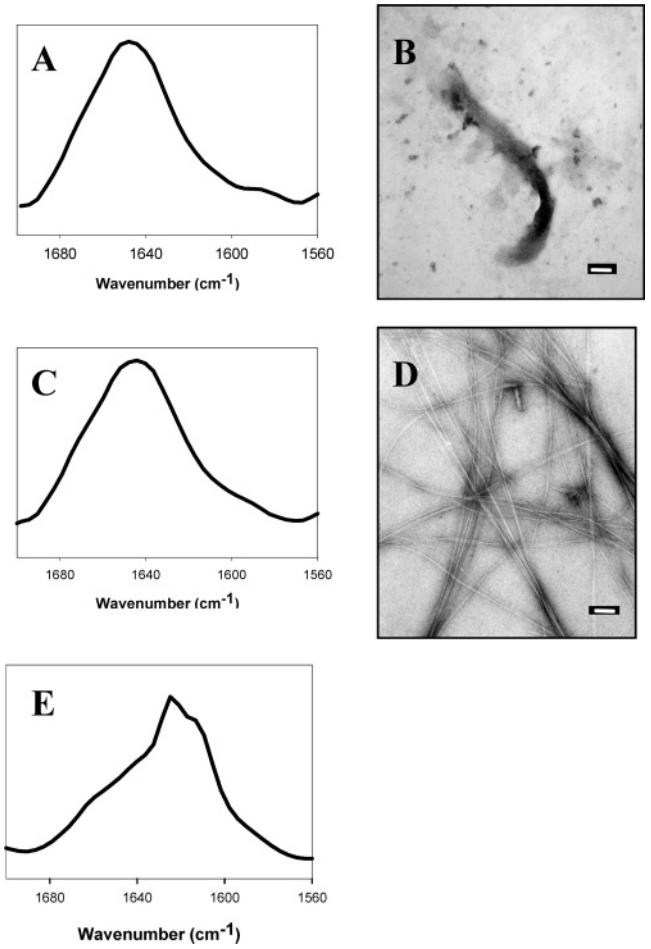

FIGURE 8: FTIR and TEM of hAmylin$_{10-19}$ F15A at pD 4.0 (±0.3) and 9.0 (±0.3). (A) FTIR spectrum at pD 4.0 (±0.3) recorded after 3 h of incubation. (B) TEM micrograph collected 3 h after sample preparation at pD 4.0 (±0.3). (C) FTIR spectrum at pD 9.0 (±0.3) recorded after 3 h of incubation. (D) TEM micrograph collected 3 h after sample preparation at pD 9.0 (±0.3). (E) FTIR spectrum at pD 9.0 (±0.3) recorded after 24 h of incubation. The scale bars represent 100 nm.

h of incubation. These data confirm that the wild-type peptide forms amyloid in a pH-dependent manner.

We also studied the effects of substituting the single aromatic residue in the 10−19 fragment. Samples of hAmylin$_{10-19}$ F15L were prepared at 6 mg/mL at pD 4.0 (±0.3) and 9.0 (±0.3) and examined by FTIR spectroscopy, TEM, and Congo Red staining. At pD 4.0 (±0.3), the His side chain is protonated and the total charge on the peptide is +2. At pD 9.0, the total charge is +1. This peptide, like the wild-type, readily forms amyloid in a pH-dependent manner. FTIR measurements were conducted at pD 4.0 (±0.3) and 9.0 (±0.3) after 3 h of incubation, conditions similar to those used for the wild type. All of the spectra recorded at pD 4.0 (±0.3) contained a broad resonance centered near 1645 cm^{-1}. The FTIR spectrum recorded after 3 h of incubation at pD 9 (±0.3) is very different. Features associated with a β-sheet structure are clearly detected (Figure 7). TEM studies confirm that amyloid formation by this peptide is pH-dependent. TEM measurements were conducted with samples that had been incubated for 3 h. Unstructured amorphous aggregates are detected by TEM at pH 4.0 (±0.3), while unbranched fibrils are observed at pH 9.0 (±0.3) (Figure 7). Samples stained with Congo Red

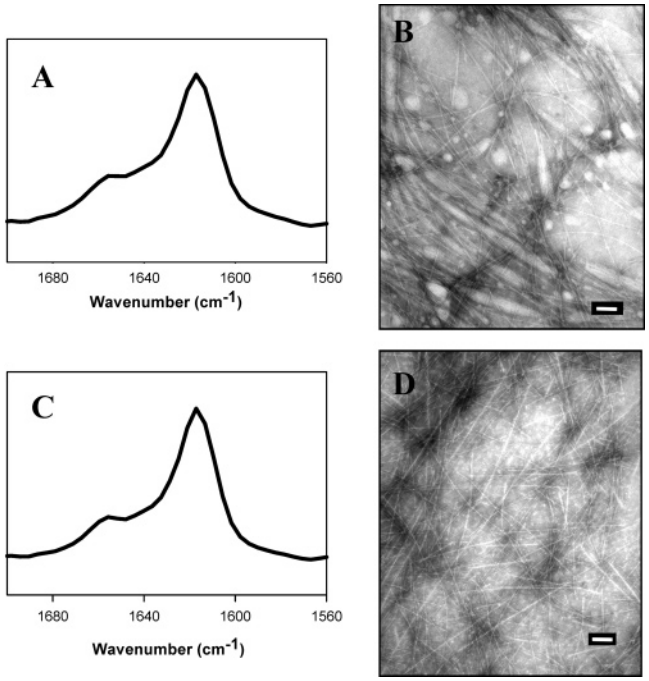

FIGURE 9: FTIR and TEM of hAmylin$_{10-19}$ H18A at pD 4.0 (±0.3) and 9.0 (±0.3). (A) FTIR spectrum at pD 4.0 (±0.3) recorded after 3 h of incubation. (B) TEM micrograph collected 3 h after sample preparation at pD 4.0 (±0.3). (C) FTIR spectrum at pD 9.0 (±0.3) recorded after 3 h of incubation. (D) TEM micrograph collected 3 h after sample preparation at pD 9.0 (±0.3). The scale bars represent 100 nm.

display strong birefringence at pD 9.0 (±0.3) but not at pD 4.0 (±0.3). Importantly, these experimental results demonstrate that the Phe-15 to Leu substitution in the 10−19 region of human Amylin does not eliminate pH-dependent amyloid formation.

A Phe-15 to Ala Substitution in hAmylin$_{10-19}$ Reduces the Tendency to Form Amyloid. Samples of hAmylin$_{10-19}$ F15A were studied under the same conditions used for the hAmylin$_{10-19}$ F15L analogue. The experimental results indicate that this peptide also undergoes pH-dependent amyloid formation, although at a much slower rate. The FTIR spectra recorded at pD 4.0 (±0.3) display a broad peak at 1645 cm^{-1} and provide no evidence for a β-sheet structure (Figure 8). Samples incubated at pD 9.0 (±0.3) for 3 h were very similar (Figure 8). Upon a longer incubation time of 24 h, the pD 9.0 (±0.3) samples develop β-sheet structure as judged by FTIR (Figure 8). TEM studies confirm that amyloid formation by this peptide is pH-dependent. TEM micrographs collected after 3 h of incubation show amorphous aggregates at pD 4.0 (±0.3) and more ordered amyloid-like fibrils at pD 9.0 (±0.3) (Figure 8). Congo Red staining further confirms pH-dependent amyloid formation. Birefringence was observed after 24 h of incubation at pD 9.0 (±0.3) but not after incubation at pD 4.0 (±0.3).

His-18 is the only residue that will titrate over the pH range studied; thus, it should be responsible for the pH-dependent effects. To confirm this, we examined the role of His-18 by studying a variant in which the residue was changed to an alanine. Samples of hAmylin$_{10-19}$ H18A were prepared at 6 mg/mL at pD 4.0 (±0.3) and 9.0 (±0.3). This peptide readily forms amyloid, and as expected, amyloid formation is not pH-dependent. FTIR measurements taken at pD 4.0 (±0.3) and 9.0 (±0.3) after 3 h of incubation give similar spectra

with an intense absorbance centered at 1625 cm^{-1}, indicating β-sheet structure (Figure 9). TEM micrographs confirm the presence of amyloid (Figure 9). The FTIR spectrum of this peptide exhibits a more intense β-sheet band than either the wild type or F15L variant. The origin of this effect is not yet clear but perhaps it indicates that a smaller side chain at position 18 favors β-sheet assembly. Further experimental studies will be required to determine the exact role of this position.

CONCLUSIONS

Our biophysical experiments demonstrate that an aromatic residue at position 23 is not required for amyloid formation by peptides derived from the 21−29 and 22−27 regions of Amylin. Peptides that contained a Phe-23 to Leu substitution were shown to form amyloid fibrils similar to the wild type. A Phe to Ala substitution in the hexapeptide, $hAmylin_{22-27}$ F23A, did have a much larger effect then a Phe to Leu substitution. Likewise, substitution of the aromatic residue at position 15 in the 10−19 region, $hAmylin_{10-19}$ F15L, did not abolish the ability to form amyloid, while a Phe to Ala substitution had a much more pronounced effect. Our observation of a large effect upon Ala substitution is in good agreement with the earlier Ala-scanning studies (*16*).

Leu and Phe are larger, more hydrophobic, and have a higher propensity to form β-sheet structure than Ala (*36*−*39*). Phe has one of the highest β-sheet propensities, while the propensity of Ala is much smaller, both as judged by statistical surveys and by thermodynamic measurements on model proteins (*36*−*38*). For example, the statistical β-sheet propensity of Phe is 1.33 using a scale where a value of 1.0 corresponds to no statistical preference to be in a β sheet (*36*−*38*). Ala, in contrast, has a low β-sheet propensity of 0.72 but a high helical propensity. The β-sheet propensity of Leu, 1.22, is noticeably higher than that of Ala, although somewhat smaller than Phe. Our studies demonstrate that the size, hydrophobicity, and/or β-sheet propensity are more important factors in these peptides than the ability to form aromatic−aromatic interactions. Along these lines Chiti and co-workers have shown that the effects of the F23A mutation can be predicted based on an empirical formula that considers charge/secondary structure propensity and hydrophobicity but not aromatic−aromatic interactions (*11*). Our results are consistent with this analysis. Recent experimental studies with a set of tetrapeptides have also highlighted the role of charge attraction and β-sheet propensity in amyloid formation (*40*). Computational studies of fragments of the Aβ peptide have emphasized the role of charge−charge interactions and hydrophobic clustering (*41*).

Aromatic−aromatic interactions could of course play a role in amyloid formation by other peptide fragments, but the work here demonstrates they are not a strict requirement in all systems. It is important to stress that even though aromatic−aromatic interactions are not a strict requirement for amyloid formation in these Amylin-derived peptides they might still play a role in either helping dictate the structure of the fibril (e.g., parallel versus antiparallel) or in the kinetics of self-assembly (*25*).

ACKNOWLEDGMENT

We thank Professor Peter Tonge for the use of his FTIR instrument and for numerous helpful discussions. We thank Professors Joseph Lauher and Frank Fowler for use of their polarizing microscope. We are also grateful to Parul Patel for many informative discussions.

REFERENCES

1. Sipe, J. D. (1994) Amyloidosis, *Crit. Rev. Clin. Lab. Sci. 31*, 325−354.
2. Lorenzo, A., Razzaboni, B., Weir, G. C., and Yankner, B. A. (1994) Pancreatic islet cell toxicity of Amylin associated with type II diabetes mellitus, *Nature 368*, 756−760.
3. Harper, J. D., and Lansbury, P. T., (1997) Models of amyloid seeding in Alzheimer's and scrapie: Mechanistic truths and physiological consequences of the time-dependent solubility of amyloid proteins, *Annu. Rev. Biochem. 66*, 385−407.
4. Prusiner, S. B., Scott, M. R., DeArmond, S. J., and Cohen, F. E. (1998) Prion protein biology, *Cell 93*, 337−348.
5. Westermark, P., Wilander, E., Hayden, D. W., O'Brian, T. D., and Johnson, K. H. (1987) Amyloid fibrils in human insulinoma and islets of langerhans of the diabetic cat are derived from a neuropeptide-like protein also present in normal islet cells, *Proc. Natl. Acad. Sci. U.S.A. 84*, 3881−3885.
6. Simmons, L. K., May, P. C., Tomaselli, K. J., Rydel, R. E., Fuson, K. S., Brigham, E. F., Wright, S., Lieberburg, I., Becker, G. W., Brems, D. N., and Li, W. Y. (1994) Secondary structure of amyloid β-peptide correlates with neurotoxic activity *in vitro*, *Mol. Pharm. 45*, 373−379.
7. Kapurniotu A. (2001) Amyloidogenicity and cytotoxicity of islet amyloid polypeptide, *Biopolymers 60*, 438−459.
8. Clark, A., Lewis, C. E., Willis, A. C., Cooper, G. J. S., Morris, J. F., Reid, K. B. M., and Turner, R. C. (1987) Islet amyloid formed from diabetes-associated peptide may be pathogenic in type II diabetes, *Lancet 2*, 231−234.
9. Cooper, G. J. S., Willis, A. C., Clark, A., Turner, R. C., Sim, R. B., and Reid, K. B. M. (1987) Purification and characterization of a peptide from amyloid-rich pancreases of type II diabetic patients, *Proc. Natl. Acad. Sci. U.S.A. 84*, 8628−8632.
10. Lopez de la Paz, M., and Serrano, L. (2004) Sequence determinants of amyloid fibril formation, *Proc. Natl. Acad. Sci. U.S.A. 101*, 87−92.
11. Chiti, F., Stefani, M., Taddei, N., Ramponi, G., and Dobson, C. M. (2003) Rationalization of the effects of mutations on peptide and protein aggregation rates, *Nature 424*, 805−808.
12. Mazor, Y., Gilead, S., Benhar, I., and Gazit, E. (2002) Identification and characterization of a novel molecular-recognition and self-assembly domain within the islet amyloid polypeptide, *J. Mol. Biol. 322*, 1013−1024.
13. Jones, S., Manning, J., Kad, N. M., and Radford, S. E. (2003) Amyloid-forming peptides from β_2-microglobulin−Insights into the mechanism of fibril formation *in vitro*, *J. Mol. Biol. 325*, 249−257.
14. Broome, B. M., and Hecht, M. H. (2000) Nature disfavors sequences of alternating polar and nonpolar amino acids: Implications for amyloidogenesis, *J. Mol. Biol. 296*, 961−968.
15. Burley, S. K., and Petsko, G. A. (1988) Weakly polar interactions in proteins, *Adv. Protein Chem. 39*, 125−189.
16. Azriel, R., and Gazit, E. (2001) Analysis of the minimal amyloid-forming fragment of the islet amyloid polypeptide, *J. Biol. Chem. 276*, 34156−34161.
17. Gazit, E. (2002) A possible role for pi-stacking in the self-assembly of amyloid fibrils, *FASEB J. 16*, 77−83.
18. Reches, M., Porat, Y., and Gazit, E. (2002) Amyloid fibril formation by pentapeptide and tetrapeptide fragments of human calcitonin, *J. Biol. Chem. 277*, 35475−35480.
19. Westermark, P., and Wilander, E. (1978) Influence of amyloid deposits on islet volume in maturity onset diabetes-mellitus, *Diabetologia 15*, 417−421.
20. Kruger, D. F., Gatcomb, P. M., and Owen, S. K. (1999) Clinical implications of amylin and amylin deficiency, *Diabetes Educ. 25*, 389−397.
21. Kahn, S. E., Andrikopoulos, S., and Verchere, C. B. (1999) Islet amyloid: A long recognized but underappreciated pathological feature of type II diabetes, *Diabetes 48*, 241−246.
22. Jaikaran, E., and Clark, A. (2001) Islet amyloid and type 2 diabetes: From molecular misfolding to islet pathophysiology, *Biochim. Biophys. Acta 1537*, 179−203.

23. Westermark, P., Engstrom, U., Johnson, K. H., Westermark, G. T., and Betsholtz, C. (1990) Islet amyloid polypeptide: Pinpointing amino acid residues linked to amyloid fibril formation, *Proc. Natl. Acad. Sci. U.S.A. 87*, 5036−5040.
24. Moriarty, D. F., and Raleigh, D. P. (1999) Effects of sequential proline substitution on amyloid formation by human Amylin 20−29, *Biochemistry 38*, 1811−1818.
25. Ashburn, T. T., and Lansbury, P. T. (1993) Interspecies sequence variations affect the kinetics and thermodynamics of amyloid formation−Peptide models of pancreatic amyloid, *J. Am. Chem. Soc. 115*, 11012−11013.
26. Ashburn, T. T., Auger, M., and Lansbury, P. T. (1992) The structural basis of pancreatic amyloid formation: Isotope-edited spectroscopy in the solid state, *J. Am. Chem. Soc. 114*, 790−791.
27. Nilsson, M. R., and Raleigh, D. P. (1999) Analysis of amylin cleavage products provides new insights into the amyloidogenic region of human amylin, *J. Mol. Biol. 294*, 1375−1385.
28. Jaikaran, E. T., Higham, C. E., Serpell, L. C., Zurdo, J., Gross, M., Clark, A., and Fraser, P. E. (2001) Identification of a novel human islet amyloid polypeptide β-sheet domain and factors influencing fibrillogenesis, *J. Mol. Biol. 308*, 515−525.
29. Goldsbury, C., Goldie, K., Pellaud, J., Seeling, J., Frey, P., Muller, S. A., Kistler, J., Cooper, G. J. S., and Aebi, U. (2000) Amyloid fibril formation from full-length and fragments of amylin, *J. Struct. Biol. 130*, 352−362.
30. Tenidis, K., Waldner, M., Bernhagen, J., Fischle, W., Bergmann, M., Weber, M., Merkle, M. L., Voelter, W., Brunner, H., and Kapurniotu, A. (2000) Identification of a penta- and hexapeptide of islet amyloid polypeptide (IAPP) with amyloidogenic and cytotoxic properties, *J. Mol. Biol. 295*, 1055−1071.
31. Zanuy, D., Ma, B., and Nussinov, R. (2003) Short peptide amyloid organization: Stabilities and conformations of the islet amyloid peptide NFGAIL, *Biophys. J. 84*, 1884−1894.
32. Zanuy, D., and Nussinov, R. (2003) The sequence dependence of fiber organization: A comparative molecular dynamics study of the islet amyloid polypeptide segments 22−27 and 22−29, *J. Mol. Biol. 329*, 565−584.
33. Zanuy, D., Porat, Y., Gazit, E., and Nussinov, R. (2004) Peptide sequence and amyloid formation: Molecular simulations and experimental study of a human islet amyloid polypeptide fragment and its analogs, *Structure 12*, 439−455.
34. Nilsson, M. R., and Raleigh, D. P. (2001) Low levels of asparagine deamidation can have dramatic effects on the aggregation of amyloidogenic peptides: Implications for the study of amyloid formation, *Protein Sci. 11*, 342−349.
35. Driscoll, M. E. (2001) Amyloid Formation by Amylin. M.S. Thesis. State University of New York at Stony Brook.
36. Chou, P. Y., and Fasman, G. D. (1978) Prediction of the secondary structure of proteins from their amino acid sequence, *Adv. Enzymol. 47*, 45−148.
37. Williams, R. W., Chang, A., Juretic, D., and Loughran, S. (1987) Secondary structure predictions and medium range interactions, *Biochim. Biophys. Acta 916*, 200−204.
38. Smith, C. K., and Regan, L. (1997) Construction and design of β-sheets, *Acc. Chem. Res. 30*, 153−161.
39. Creighton, T. E. (1993) *Proteins: Structures and Molecular Properties*, 2nd ed., W. H. Freeman and Co., New York.
40. Tjernberg, L., Hosia, W., Bark, N., Thyberg, J., and Johansson, J. (2002) Charge attraction and β-propensity are necessary for amyloid fibril formation from tetrapeptides, *J. Biol. Chem. 277*, 43243−43246.
41. Klimov, D. K., and Thirumalai, D. (2003) Dissecting the assembly of Aβ_{16-22} amyloid peptides into antiparallel β sheets, *Structure 11*, 295−307.

BI048812L